Quantum phase transitions and pairing in Strongly Attractive Fermi Atomic Gases

M.T. Batchelor
Department of Theoretical Physics and Mathematical Sciences Institute

In collaboration with **X.W. Guan, C. Lee and M. Bortz**

Outline

I. Introduction

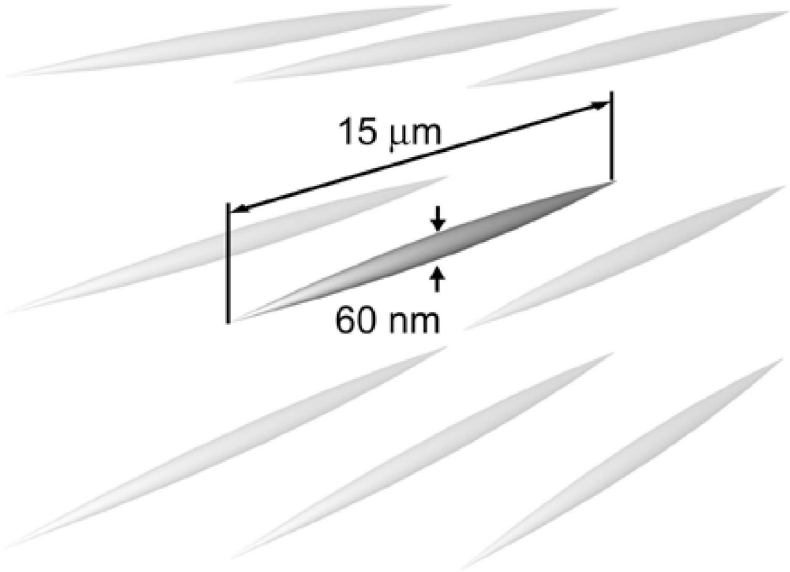

- trapped 1D gases in 2D optical lattice
- anisotropic confinement or Feshbach resonance
- experiments for the 1D Bose gas: Greiner(Nature), Paredes(Nature), Pollet(PRL), Weiss(PRL)
- quasi 1D Fermi gas: Moritz(PRL)
- 3D Fermi superfluid: Zwierlein(Science,Nature);Partridge(Science)
- BCS-BEC crossover: Regal(PRL);Zwierlein(PRL)
- spin waves: Lewandowski(PRL), McGuirk(PRL)

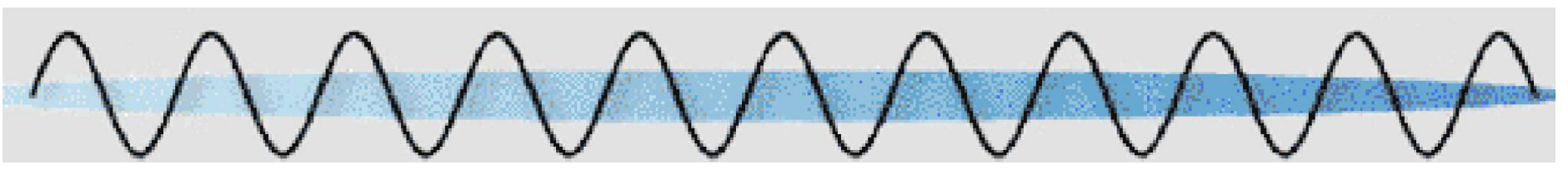

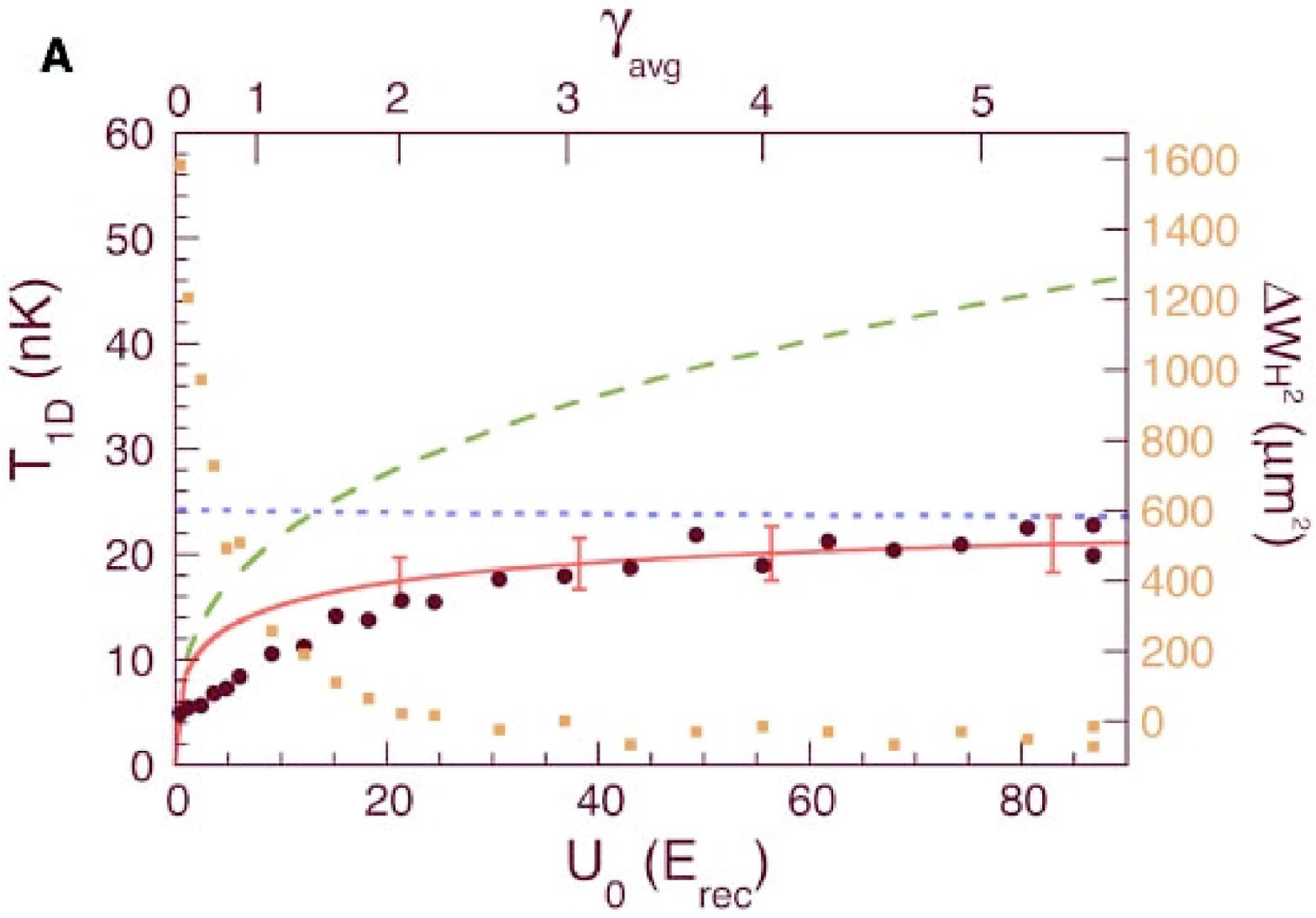

Tonks-Girardeau gas: $\gamma > 1$ for ^{87}Rb (Weiss et al. Nature 305 2004 1125)

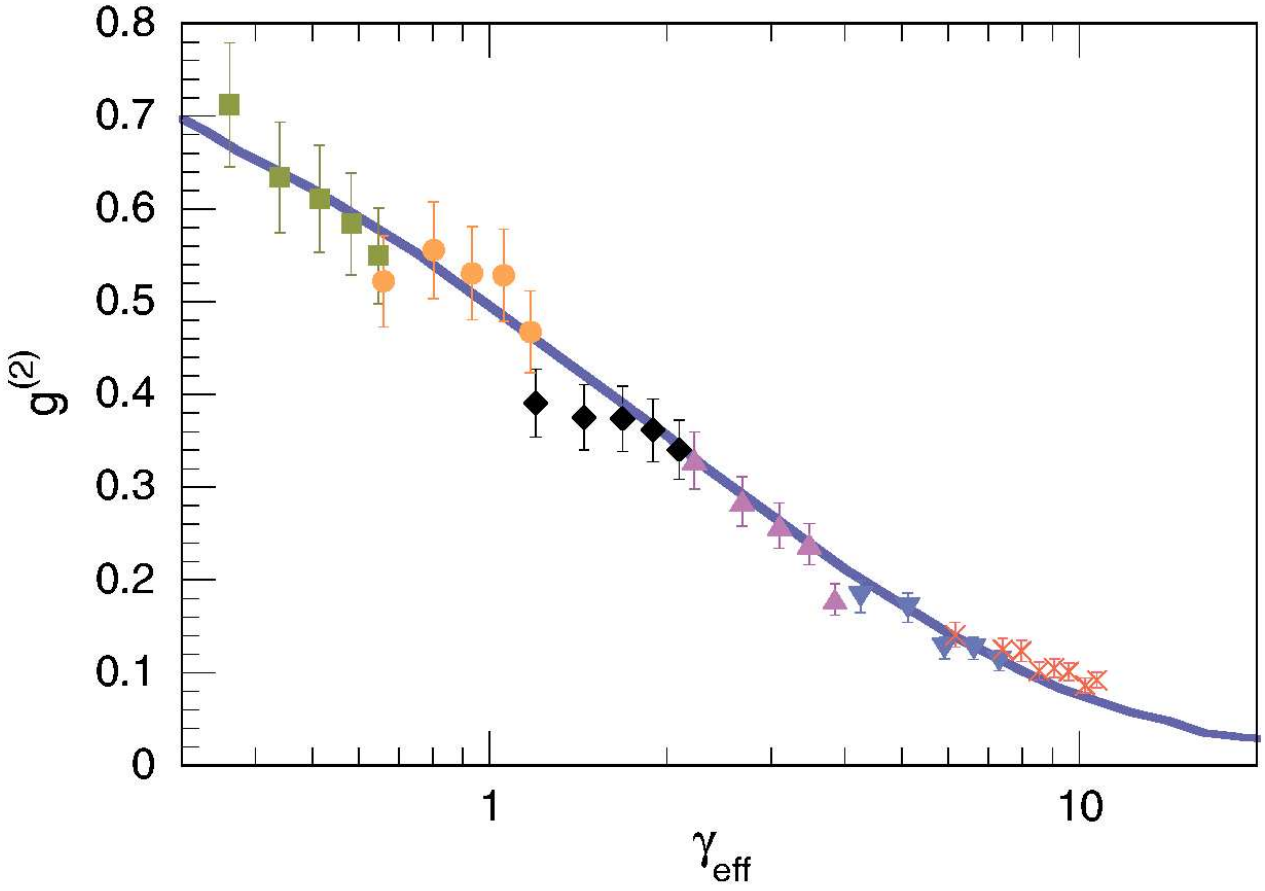

The local pair correlation function vs the coupling strength. The solid line is the 1D Bose gas theory. The points are experimental measurements. From T. Kinoshita, T. Wenger and D. S. Weiss, PRL 95, 190406 (2005).

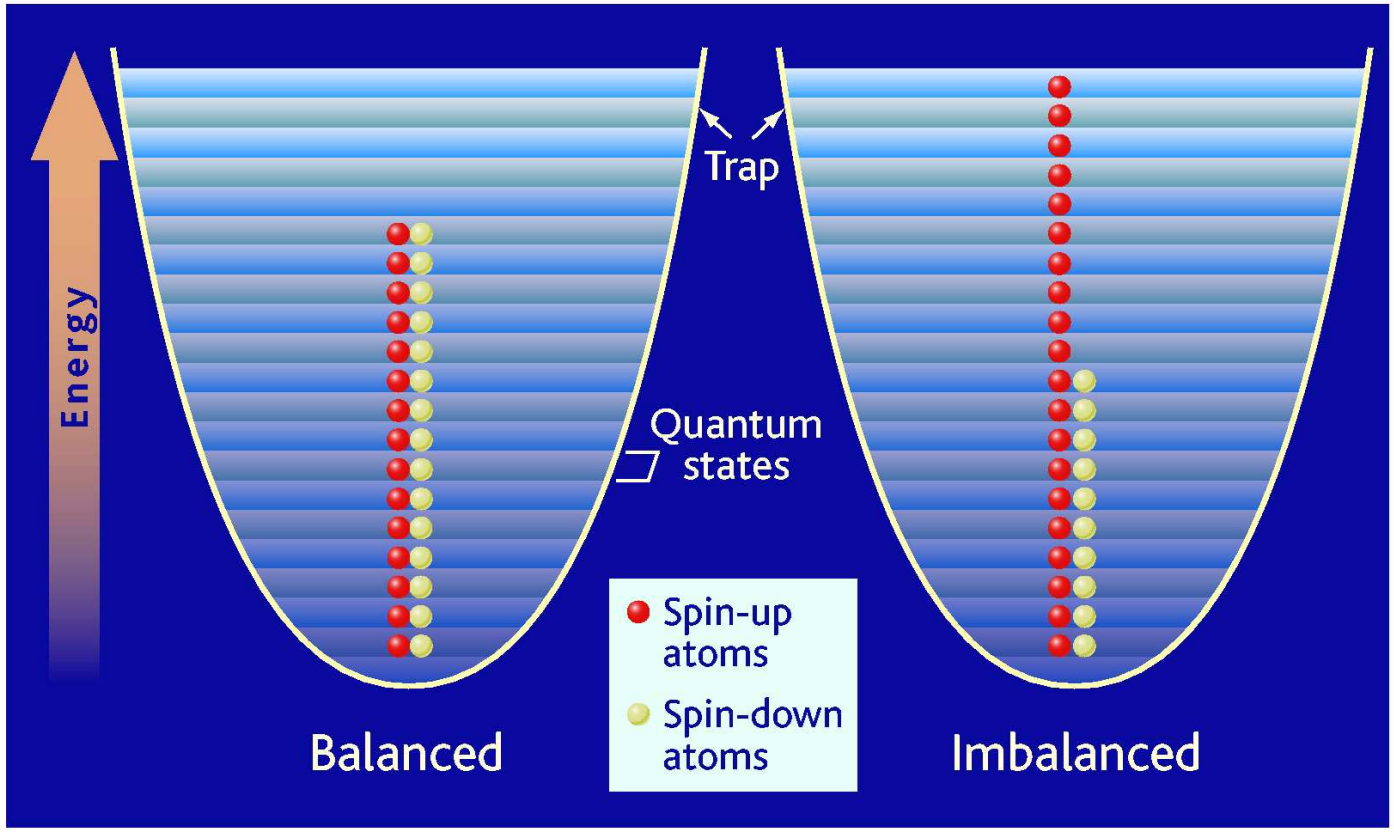

Find a partner. When atoms spinning one way outnumber those spinning the other, they still can pair and flow freely—perhaps like matter in a neutron star.

In conventional superconductors the chemical potentials of the two spin states are equal. Imbalanced chemical potentials for the two species may trigger several mechanisms: a quantum phase transition from a BCS superfluid to a normal state; a LOFF phase, etc.

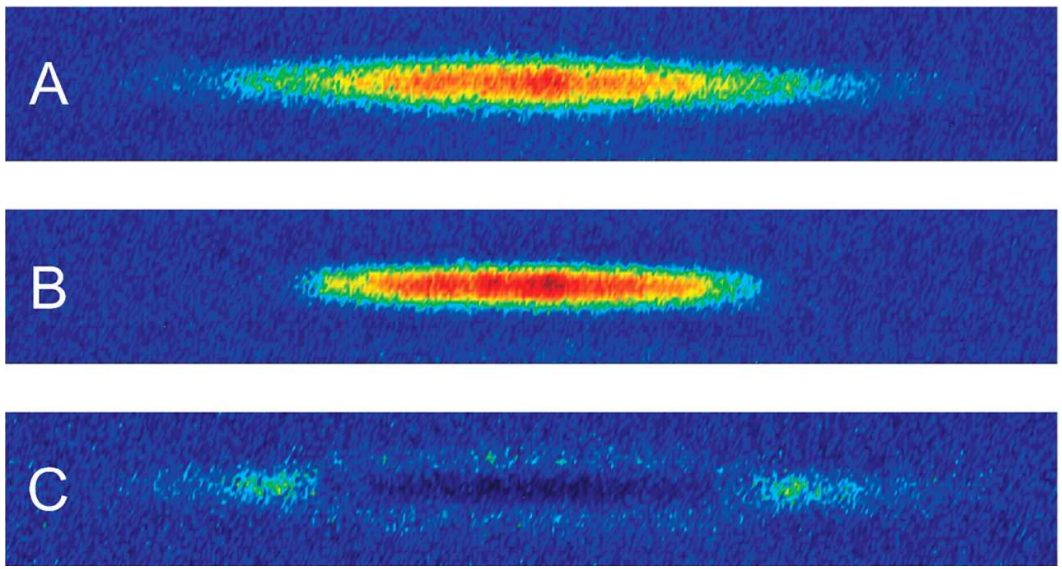

- Pairing and Phase Separation in the Polarized Fermi Gas (Partridge et al.)
- two hyperfine states of ^{6}Li:
  $|1\rangle = |F = \frac{1}{2}, m_f = \frac{1}{2}\rangle$
  $|2\rangle = |F = \frac{1}{2}, m_f = -\frac{1}{2}\rangle$
- The gas has separated into a uniformly paired inner core surrounded by a shell of the excess unpaired atoms

II. 1D two-component Fermi gas

Hamiltonian

$$\begin{aligned}
\mathcal{H} &= \mathcal{H}_0 + \mathcal{H}_i + \mathcal{H}_c \\
\mathcal{H}_0 &= \sum_{j=1,2} \int \psi_j^+(x) \left(-\frac{\hbar^2}{2m}\frac{d^2}{dx^2} + V(x) \right) \psi_j(x) dx \\
\mathcal{H}_i &= g_{1D} \int \psi_1^+(x)\psi_2^+(x)\psi_2(x)\psi_1(x) dx \\
\mathcal{H}_c &= \frac{\Omega}{2} \int \left(\psi_2^+(x)\psi_1(x) + \psi_1^+(x)\psi_2(x) \right) dx
\end{aligned}$$

Hamiltonian

$$\begin{aligned}
\mathcal{H} &= \sum_{j=\downarrow,\uparrow} \int \phi_j^+(x) \left(-\frac{\hbar^2}{2m}\frac{d^2}{dx^2} + V(x) \right) \phi_j(x) dx \\
&+ g_{1D} \int \phi_\downarrow^+(x)\phi_\uparrow^+(x)\phi_\uparrow(x)\phi_\downarrow(x) dx \\
&- \frac{\Omega}{2} \int \left(\phi_\uparrow^+(x)\phi_\uparrow(x) - \phi_\downarrow^+(x)\phi_\downarrow(x) \right) dx
\end{aligned}$$

transformation

$$\phi_\downarrow = (\psi_1 + \psi_2)/\sqrt{2}; \quad \phi_\uparrow = (\psi_1 - \psi_2)/\sqrt{2}$$

QM Hamiltonian

$$\mathcal{H} = -\frac{\hbar^2}{2m}\sum_{i=1}^{N}\frac{\partial^2}{\partial x_i^2} + g_{1D}\sum_{1\le i<j\le N}\delta(x_i - x_j)$$

Wavefunctions

$$\psi(x_1, \cdots, x_N) = \sum_{P,Q} A_{Q1,\cdots,QN}(P|Q)\exp(i\sum_j k_{Pj}x_{Qj})$$

Energy

$$E = \frac{\hbar^2}{2m}\sum_{j=1}^{N} k_j^2$$

Bethe Ansatz eqns

$$\exp(ik_jL) = \prod_{\ell=1}^{M}\frac{k_j - \Lambda_\ell + ic/2}{k_j - \Lambda_\ell - ic/2},$$

$$\prod_{\ell=1}^{N}\frac{\Lambda_\alpha - k_\ell + ic/2}{\Lambda_\alpha - k_\ell - ic/2} = -\prod_{\beta=1}^{M}\frac{\Lambda_\alpha - \Lambda_\beta + ic}{\Lambda_\alpha - \Lambda_\beta - ic}$$

III. Groundstate properties

$L|c| \ll 1$ — the system is described by weakly bound Cooper pairs. M bound states: $k_\alpha^{\rm p} \approx \Lambda_\alpha \pm {\rm i}\sqrt{c/L}$; $N-2M$ unpaired fermions: k_i are real.

$$\frac{L}{c} \approx \frac{2n_j\pi}{c\,k_j} + \frac{1}{k_j^2} + \sum_{\alpha=1}^{(M-1)/2} \frac{2}{k_j^2-\Lambda_\alpha^2}, \qquad n_j = (M+1)/2, \cdots (N-M-1)/2$$

$$\frac{L}{c} \approx \frac{2n_\alpha\pi}{c\Lambda_\alpha} + \frac{3}{2\Lambda_\alpha^2} + \sum_{\beta=1}^{(M-1)/2} \frac{2}{\Lambda_\alpha^2-\Lambda_\beta^2} + \sum_{j=(M+1)/2}^{(N-M-1)/2} \frac{1}{\Lambda_\alpha^2-k_j^2}, \quad n_\alpha = 1, \cdots, \frac{(M-1)}{2}$$

energy

$$\frac{E}{L} \approx \frac{\hbar^2}{2m}\left(\frac{c}{2}n^2(1-P^2) + \frac{\pi^2}{12}n^3 + \frac{\pi^2}{4}n^3P^2\right), \quad P = \frac{N_\uparrow - N_\downarrow}{N}$$

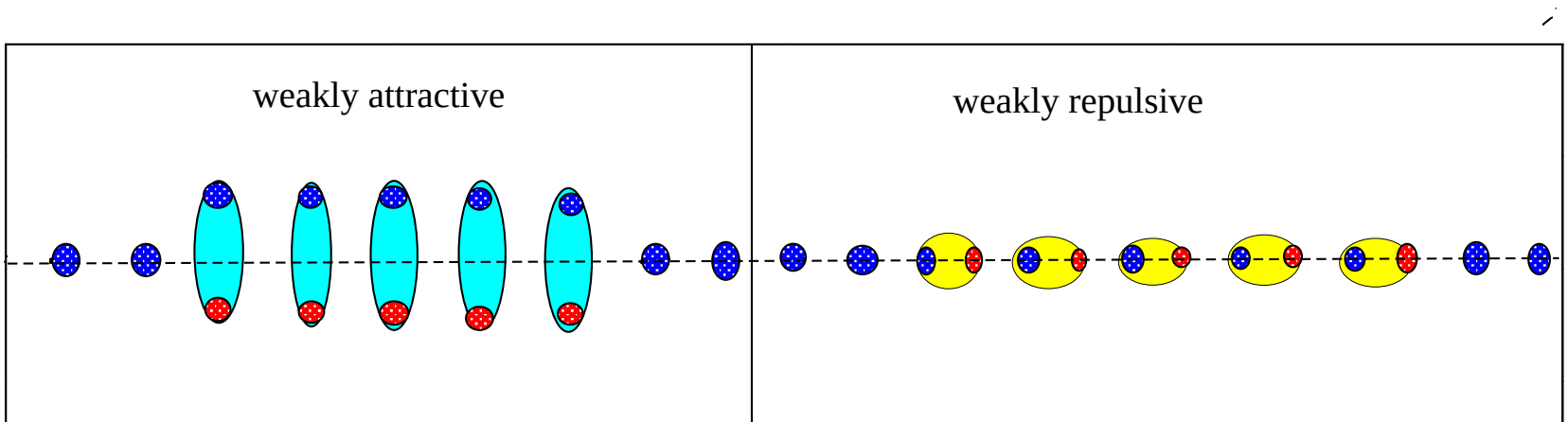

strong interaction

the bound states: $k_i^{(\mathrm{p})} \approx \frac{n_i \pi}{L}\left(1+\frac{M}{L|c|}+\frac{2(N-2M)}{L|c|}\right) \pm \frac{1}{2}\mathrm{i}c$ for $n_i = 0, \pm 1, \ldots, \pm\frac{1}{2}(M-1)$; Unpaired fermions: $k_j^{(\mathrm{u})} \approx \frac{n_j \pi}{L}\left(1+\frac{4M}{L|c|}\right)$ with $n_j = \pm 1, \pm 3 \ldots, \pm(N-2M-1)$.

energy

$$\frac{E}{L} \approx \frac{\hbar^2 n^3}{2m}\left\{-\frac{(1-P)\gamma^2}{4}+\frac{P^3\pi^2}{3}\left(1+\frac{4(1-P)}{|\gamma|}\right) + \frac{\pi^2(1-P)^3}{48}\left(1+\frac{(1-P)}{|\gamma|}+\frac{4P}{|\gamma|}\right)\right\}$$

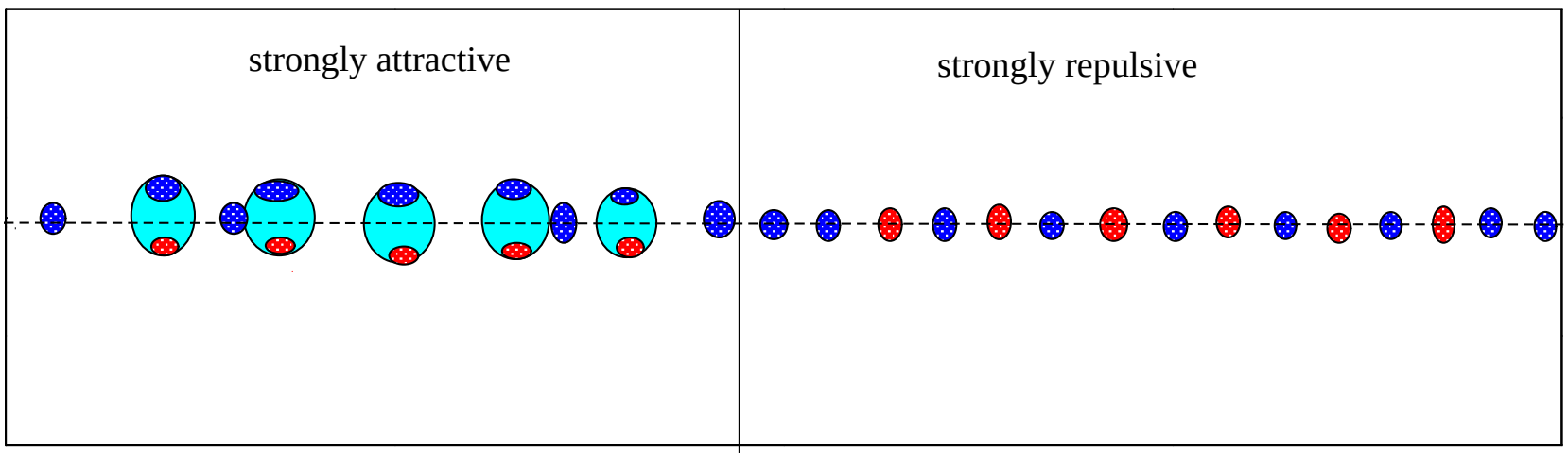

BAEs for $c > 0$

$$\rho(k) = \frac{1}{2\pi} + \frac{1}{2\pi}\int_{-B}^{B} \frac{c\sigma(\lambda)}{c^2/4+(k-\lambda)^2} d\lambda$$

$$\sigma(\lambda) = \frac{1}{2\pi}\int_{-Q}^{Q} \frac{c\rho(k)}{c^2/4+(\lambda-k)^2} dk - \frac{1}{2\pi}\int_{-B}^{B} \frac{2c\sigma(\lambda')}{c^2+(\lambda-\lambda')^2} d\lambda'$$

$$E/L = \int_{-Q}^{Q} k^2\rho(k)dk,\ n = \int_{-Q}^{Q} \rho(k)dk,\ n_\downarrow = \int_{-B}^{B} \sigma(\Lambda)d\Lambda$$

BAEs for $c < 0$

$$\rho(k) = \frac{1}{2\pi} - \frac{1}{2\pi}\int_{-Q}^{Q} \frac{|c|\sigma(\Lambda)}{c^2/4+(k-\Lambda)^2} d\Lambda$$

$$\sigma(\Lambda) = \frac{1}{\pi} - \frac{1}{2\pi}\int_{Q}^{Q} \frac{|c|\rho(k)}{c^2/4+(\Lambda-k)^2} dk - \frac{1}{2\pi}\int_{-B}^{B} \frac{2|c|\sigma(\Lambda')d\lambda}{c^2+(\Lambda-\Lambda')}$$

$$E/L = \int_{-Q}^{Q} k^2\rho(k)dk + \int_{-B}^{B} (2\Lambda^2 - \frac{c^2}{2})\sigma(\Lambda)d\Lambda$$

$$n = 2\int_{-B}^{B} \sigma(\Lambda)d\Lambda + \int_{-Q}^{Q} \rho(k)dk,\quad n_\uparrow - n_\downarrow = \int_{-Q}^{Q} \rho(k)dk$$

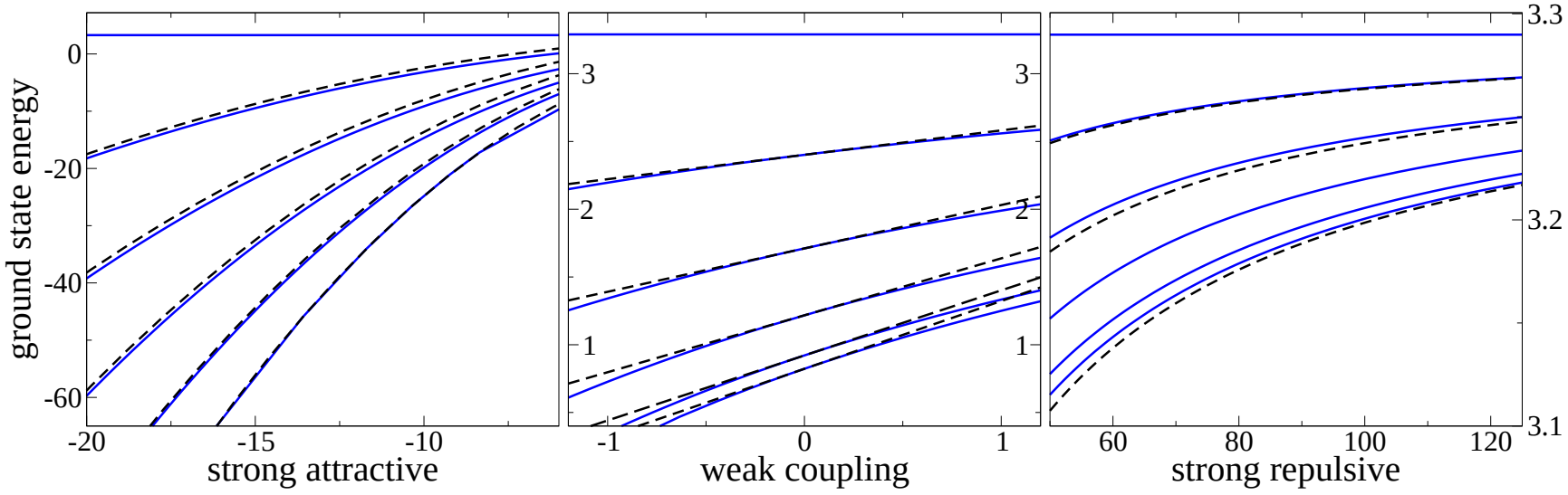

Ground state energy in units of $\hbar^2 n^2/(2m)$ vs interaction strength γ for different polarizations. Dashed lines compare the analytic approximations with the numerical solution of the integral equations (solid lines) in the different coupling regimes. The curves shown are for $P = 1, 0.8, 0.6, 0.4, 0.2, 0$ (top to bottom). **Iida-Wadati Series**: T. Iida and M. Wadati, J. Phys. Soc. Jpn. **74**, 1724 (2005); **Asymptotic Bethe ansatz solutions**: M.T. Batchelor, M. Bortz, X.W. Guan and N. Oelkers, J. Phys. Conf. Series **42**, 5 (2006).

IV.Phase transitions for attractive interaction

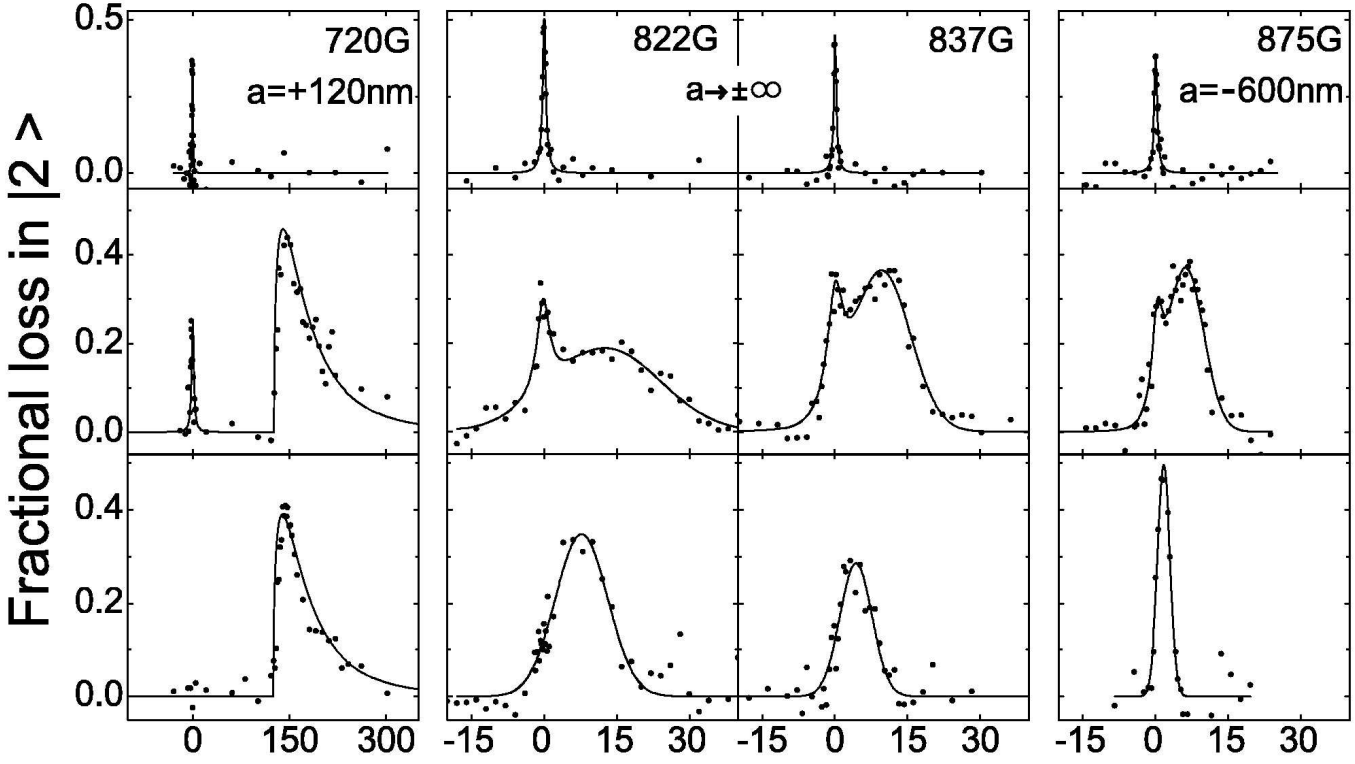

Observation of the pairing gap in strongly interacting Fermi Gas: ultracold two-component gas of ^{6}Li. RF spectra for various magnetic fields and different degrees of evaporative cooling: the peak at zero RF is caused by free atoms; a peak shifted to the right from zero for low T, corresponding to paired atoms. C. Chin et al. Science 305, 1128 (2004)

IV.Phase transitions for attractive interaction

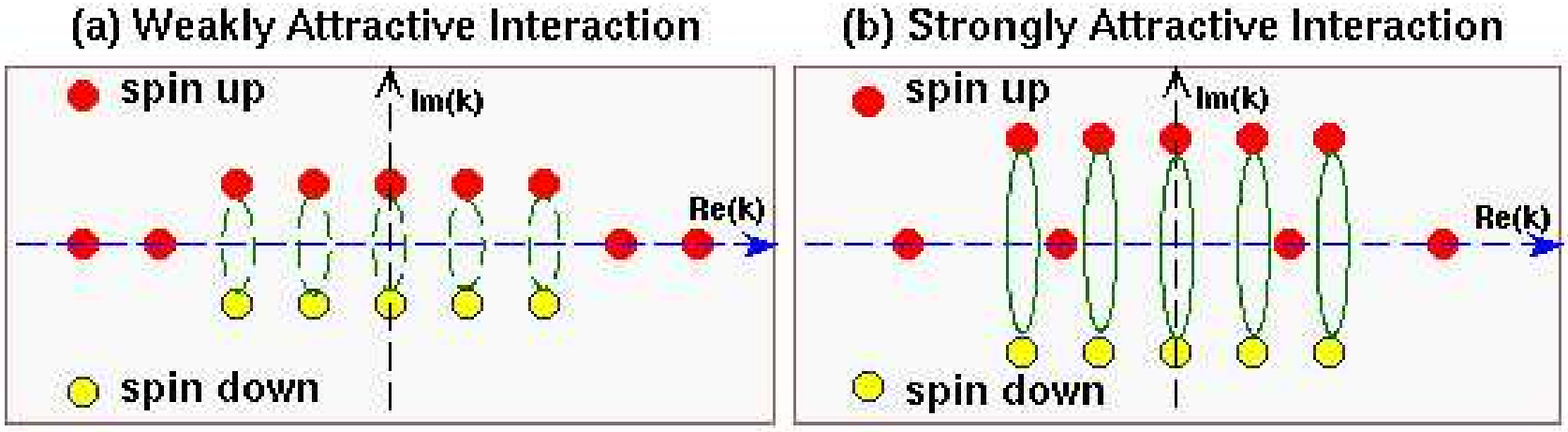

Ultracold atomic gases provide exceptionally clean quantum systems that allow us to observe BCS pairing and superfluidity. For equal number of fermions with up- and down- spin states, two fermions with opposite momentum and spin state can form a BCS Cooper pair at the Fermi surface. The BCS pairs can be thought of as composite bosons that undergo BEC. However, the nature of pairing and superfluidity in strongly interacting systems of fermionic atoms with population imbalance is very subtle and intriguing. Cooper-pairing is a momentum-space phenomenon. Therefore, the pairing signature in 1D interacting Fermi gases with strongly attractive interaction should shed light on understanding the Fermi superfluidity to normal phase transition in higher dimensions.

Thermodynamical Bethe ansatz(TBA): Yang and Yang introduced the TBA in treating the thermodynamics of the one-dimensional boson model with delta function interaction. In general, at $T = 0$ there are no holes in the ground state root distributions. For $T \neq 0$, complex Bethe roots form strings characterizing the excitations. The string hypothesis has been developed to classify the many permissible bound state solutions to the Bethe equations. The equilibrium states satisfy the condition of minimizing the Gibbs free energy $G = E - \mu N - HM^z - TS$.

$T \to 0$

$$\begin{aligned}
\epsilon^{\mathrm{b}}(\Lambda) &= 2(\Lambda^2 - \mu - \frac{c^2}{4}) - \int_{-B}^{B} a_2(\Lambda - \Lambda')\epsilon^{\mathrm{b}-}(\Lambda')d\Lambda' \\
&\quad - \int_{-Q}^{Q} a_1(\Lambda - k)\epsilon^{\mathrm{u}-}(k)dk \\
\epsilon^{\mathrm{u}}(k) &= (k^2 - \mu - \frac{H}{2}) - \int_{-B}^{B} a_1(k - \Lambda)\epsilon^{\mathrm{b}-}(\Lambda)d\Lambda \\
G &= \frac{1}{\pi}\int_{-B}^{B} \epsilon^{\mathrm{b}-}(\Lambda)d\Lambda + \frac{1}{2\pi}\int_{-Q}^{Q} \epsilon^{\mathrm{u}-}(k)dk
\end{aligned}$$

$\epsilon^{\mathrm{b,u}}$: the dressed energies for the paired fermions and unpaired fermions, respectively. The TBA provides a clear configuration for band fillings with respect to the external field H and chemical potential μ (see, Takahashi's book).

groundstate

$$E \approx \frac{\hbar^2 n^3}{2m}\left\{-\frac{(1-P)\gamma^2}{4}+\frac{\pi^2(1-P)^3}{48}\left(1+\frac{(1-P)}{|\gamma|}+\frac{4P}{|\gamma|}\right)-\frac{P^3\pi^2}{3}\left(1+\frac{4(1-P)}{|\gamma|}\right)\right\}$$

magnetization

$$\frac{H}{2} \approx \frac{\hbar^2}{2m}\left\{\frac{c^2}{4}+4\pi^2(M^z)^2\left(1+\frac{4(n-2M^z)}{|c|}-\frac{8M^z}{3|c|}\right)-\frac{\pi^2}{16}\left(n-2M^z\right)^2\left(1+\frac{8M^z}{|c|}\right)\right\}$$

cf $2\pi\hbar\delta = \epsilon_{\rm b} + \Delta E_{\rm k}$, (Moritz et al. PRL 05)

critical fields

$$H_{c1} \approx \frac{\hbar^2 n^2}{2m}\left(\frac{\gamma^2}{2}-\frac{\pi^2}{8}\right)$$

$$H_{c2} \approx \frac{\hbar^2 n^2}{2m}\left(\frac{\gamma^2}{2}+2\pi^2(1-\frac{4}{3|\gamma|})\right)$$

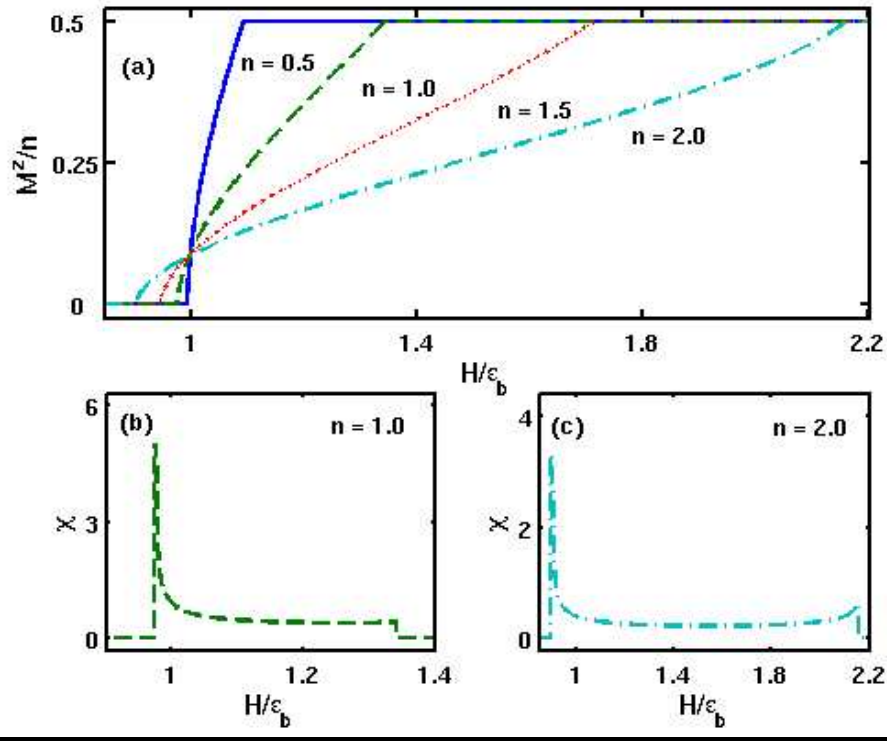

Magnetization M^z vs magnetic field H (in the units of $\frac{\hbar^2}{2m}$). The inset shows the susceptibility vs the field H. In the vicinities of H_{c1} and H_{c2} the phase transitions are determined by the linear field-dependent relations $M^z \approx \frac{2(H-H_{c1})}{n\pi^2}(1+2|\gamma^{-1}|)$ and $M^z \approx \frac{n}{2}\left(1-\frac{(H_{c2}-H)}{4n^2\pi^2}(1+\frac{10}{3|\gamma|})\right)$, respectively. The susceptibility decays exponentially in the vicinity of critical field H_{c1} then it approaches to a constant for $H < H_{c2}$.

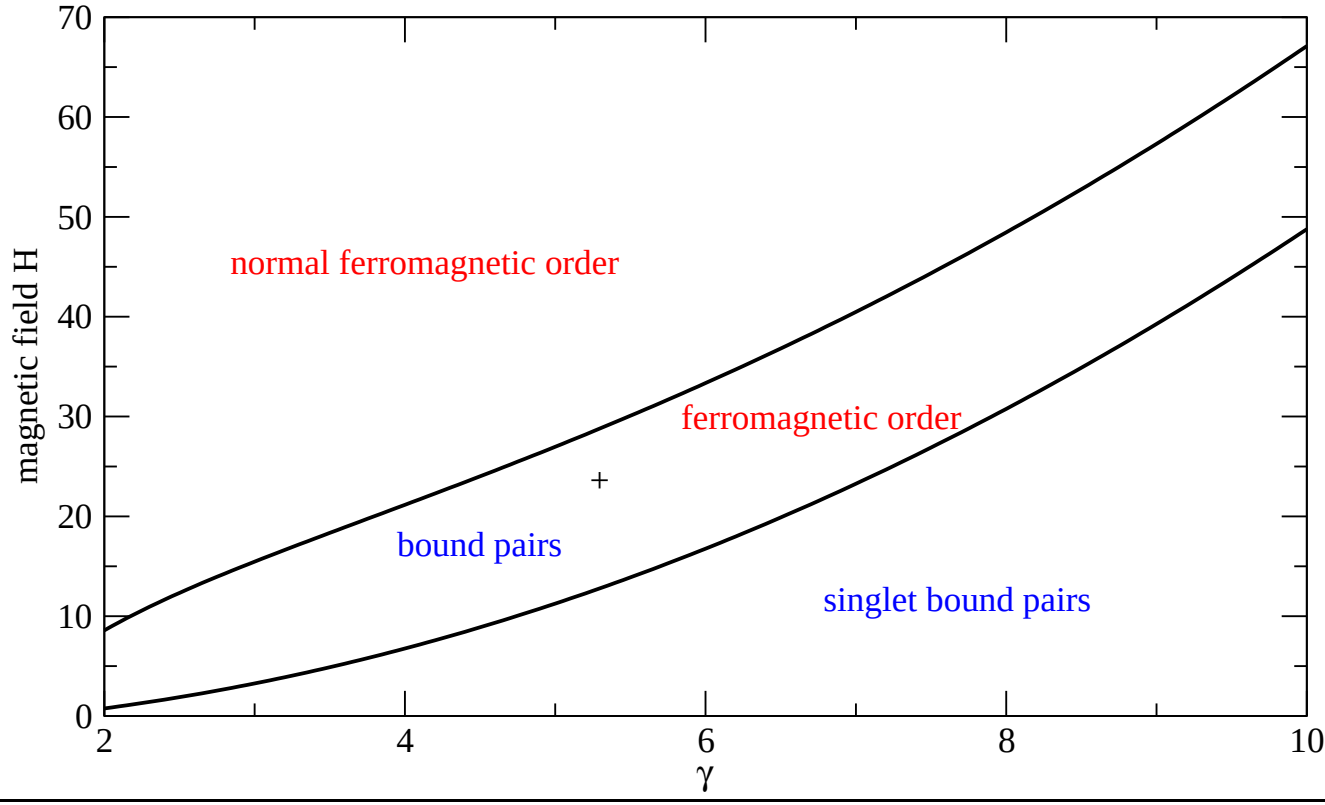

At zero temperature, the bound pairs of fermions form a singlet ground state for the field $H < H_{c1}$. However, for $H > H_{c2}$, a normal ferromagnetic order occurs. A "new phase of matter" is found for the field $H_{c1} < H < H_{c2}$, where the singlet bound state coexists with the ferromagnetic order. The phase transitions at the critical points are of second order.

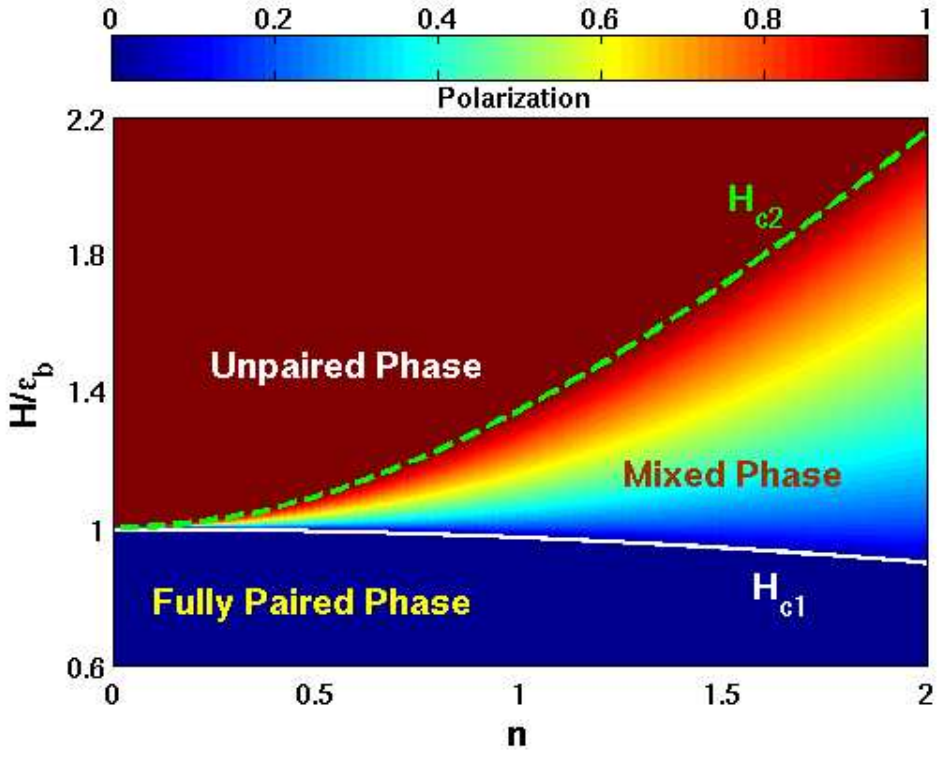

Phase diagram in the $H - n$ plane for the particular value $|c| = 10$: As $n \to 0$, the two critical fields approach the binding energy ϵ_b. The two critical fields have opposite monotonicity: H_{c1} decreases with increasing n whereas H_{c2} increases with n. Thus, for sufficiently large centre-density, the system has subtle segments: the mixed phase lies in the centre and the fully paired phase (or the fully unpaired phase) sits in the two outer wings for $H < \epsilon_b$ (or $H > \epsilon_b$).

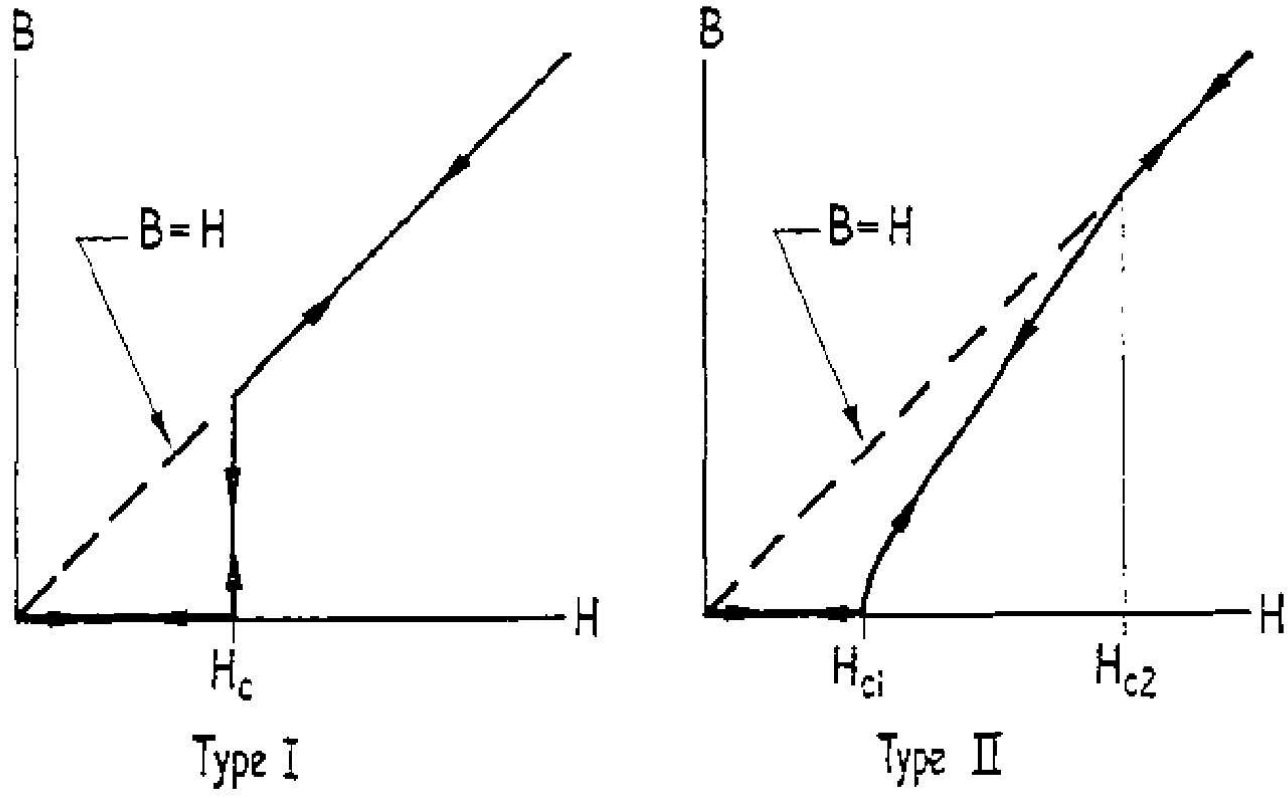

The phase diagram for the 1D Fermi gas with strong attractive interaction is reminiscent of the quantum phase transitions in type II superconductors: a Meissner phase occurs for external magnetic field less than the lower critical field; between the lower and the upper critical fields the superconducting state and a magnetic field coexist; a normal conducting phase occurs when the field exceeds the upper critical field.

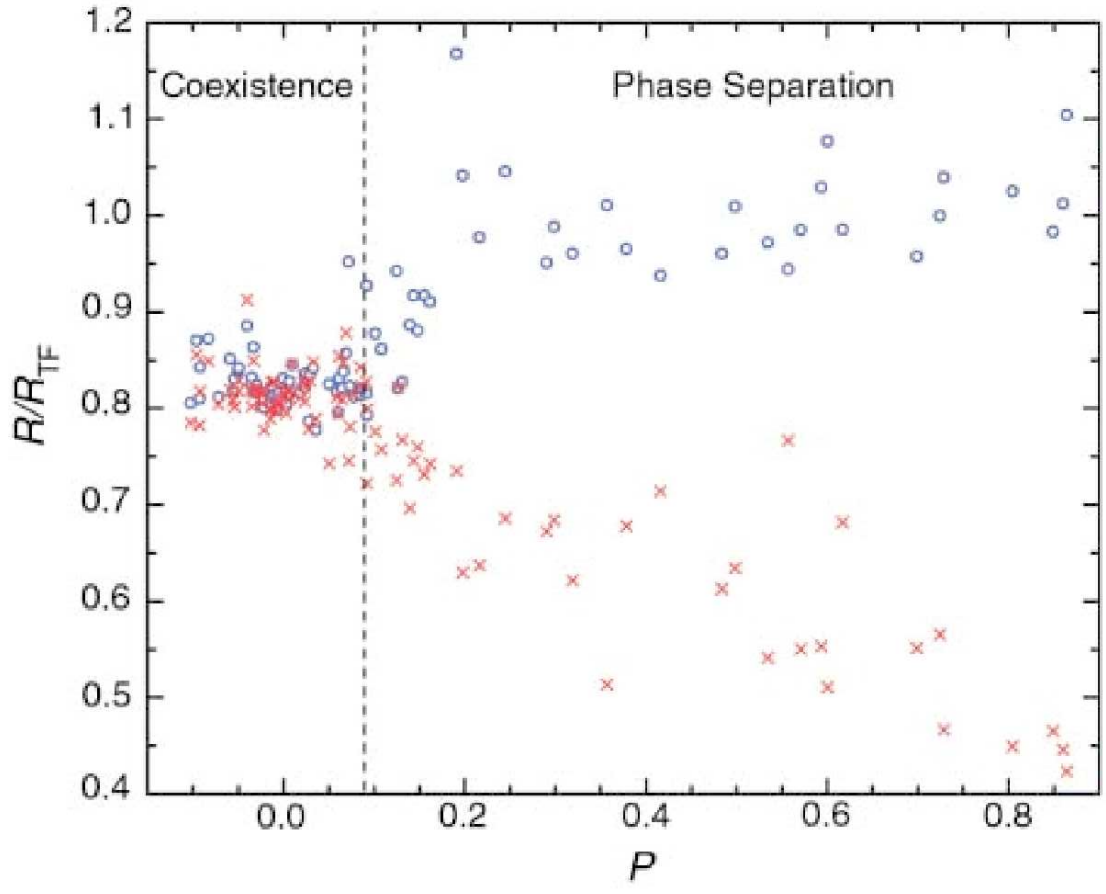

R/R_{TF} versus P: the ratios of the measured axial radius to T-F radius are shown as blue open circles for state $|1\rangle$ and red crosses for state $|2\rangle$. (Partridge et al. Science 06). In the 1D Fermi gas, the effective chemical potentials for fermions with down-spin $\mu^{\downarrow} = \mu - H/2$ and for fermions with up-spin $\mu^{\uparrow} = \mu + H/2$, which give the same signature as in the figure.

chemical potential: bound pairs: $\mu^{\mathrm{b}} = \mu + \epsilon_{\mathrm{b}}/2$; unpaired fermions: $\mu^{\mathrm{u}} = \mu + H/2$

$$\mu^{\mathrm{b}} \approx \frac{\hbar^2 n^2 \pi^2}{2m}\left\{\frac{(1-P)^2}{16}\left(1+\frac{4(1-P)}{3|\gamma|}+\frac{4P}{|\gamma|}\right)+\frac{4P^3}{3|\gamma|}\right\}$$

$$\mu^{\mathrm{u}} \approx \frac{\hbar^2 n^2 \pi^2}{2m}\left\{P^2\left(1+\frac{4(1-P)}{|\gamma|}\right)+\frac{(1-P)^3}{12|\gamma|}\right\}$$

Fermi momentum

$$K_B \approx \frac{n\pi(1-P)}{4}\left(1+\frac{(1-P)}{2|\gamma|}+\frac{2P}{|\gamma|}\right)$$

$$K_Q \approx n\pi P\left(1+\frac{2(1-P)}{|\gamma|}\right)$$

GES distribution

$$\sum_j (w_j \delta_{i,j} + \beta_{i,j}) n_j = 1,\ n_i = N_i/G_i,\ \beta_{i,j} = \alpha_{i,j} G_j/G_i$$

$$(1+w_i) \prod_j \left(\frac{w_j}{1+w_j} \right)^{\alpha_{j,i}} = e^{(\epsilon_i - \mu_i)/K_B T}$$

TBA

$$\epsilon(\Lambda) = 2(\Lambda^2 - \mu - \frac{c^2}{4}) + T \int_{-\infty}^{\infty} a_2(\Lambda - \Lambda') \ln \left(1 + e^{-\epsilon(\Lambda')/K_B T}\right) d\Lambda'$$

TBA result

$$n(\epsilon) = \frac{1}{\alpha(1 - e^{(\epsilon - 2\bar{\mu})/K_B T})},\ \alpha = 1 + 1/(2|\gamma|)$$

$$\bar{\mu} = \mu_0 \left[1 + \frac{16\tau^2}{3\pi^2}(1 - \frac{2}{|\gamma|}) + \frac{1024\tau^4}{9\pi^4}(1 - \frac{4}{|\gamma|}) + O(t^6)\right]$$

Ideal GES

$$n(\epsilon) = \frac{1}{\alpha + w(\epsilon)},\ w^{\alpha}(\epsilon)(1 + w(\epsilon))^{1-\alpha} = e^{\frac{\epsilon - 2\bar{\mu}}{K_B T}}$$

$$\bar{\mu} = \mu_0 \left[1 + \frac{16\tau^2}{3\pi^2\alpha^3} + \frac{192\zeta(3)\tau^3}{\pi^6\alpha^5|\gamma|} + \frac{1024\tau^4}{9\pi^4\alpha^6} + O(t^6)\right]$$

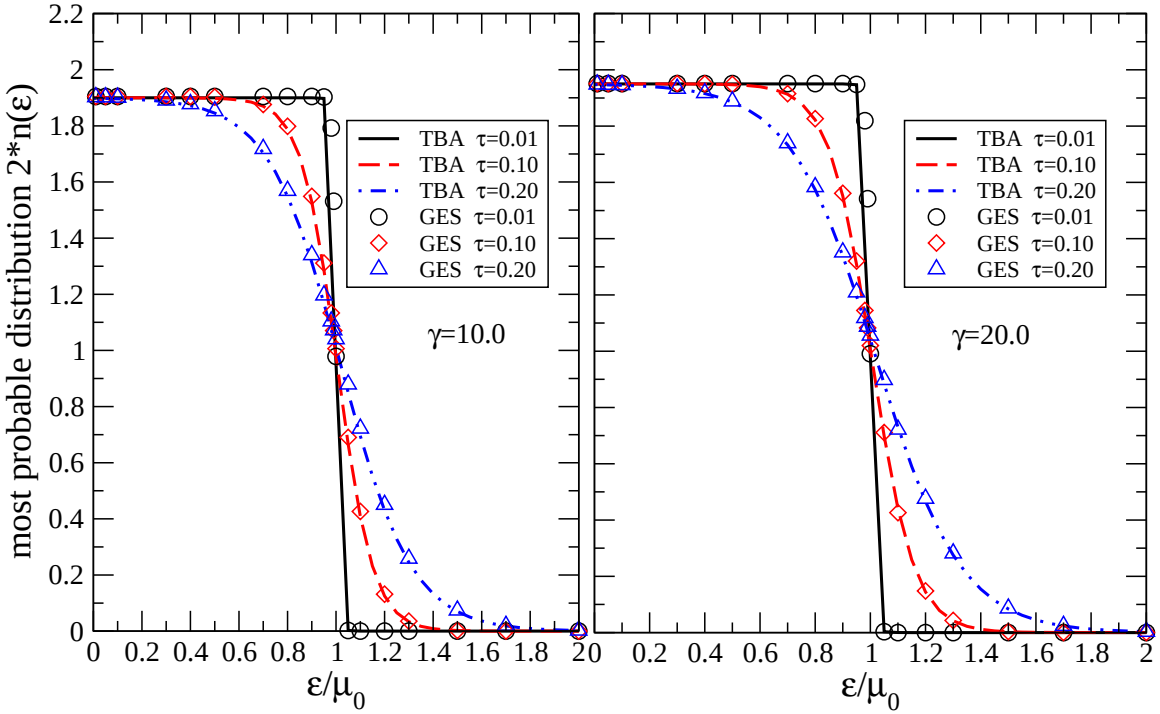

Comparison between distribution profiles derived from TBA and GES for the values $|\gamma| = 10, 20$ at different values of the degeneracy temperature $\tau = K_B T / T_d$. Attractive interaction results in a more exclusive state than the pure Fermi-Dirac statistics. The lines show the TBA distribution function. The symbols show the most probable distribution evaluated from the GES result. The energy and specific heat are given by $E = E_0 \left[1 + \frac{16\tau^2}{\pi^2}(1 - \frac{2}{|\gamma|})\right]$ and $c_v = \frac{nK_B\tau}{3}\left(1 - \frac{1}{|\gamma|}\right)$ (cf Kinast et al. Science 05) and Bhaduri et al. EPL 06).

V. Conclusion

- Attractive Fermi gas: a new phase of matter induced by an interior gap has been studied; the phase diagram, critical fields and magnetic properties have been obtained. The phase diagram is reminiscent of that of type II superconductors.

- F. D. M. Haldane, Phys. Rev. Lett. **67**, 937 (1991); Y.-S. Wu, Phys. Rev. Lett. **73**, 922 (1994).
- Z. N. C. Ha, Phys. Rev. Lett. **73**, 1574 (1994); S. B. Isakov, Phys. Rev. Lett. **73**, 2150 (1994); M. Wadati, J. Phys. Soc. Jpn. **64**, 1552 (1995).
- T. Iida and M. Wadati, J. Phys. Soc. Jpn. **74**, 1724 (2005); M.T. Batchelor, M. Bortz, X.W. Guan and N. Oelkers, J. Phys. Conf. Series **42**, 5 (2006).
- M. T. Batchelor, X.-W. Guan and N. Oelkers, Phys. Rev. Lett. **96**, 210402 (2006); M. T. Batchelor and X.-W. Guan, Phys. Rev. B **74**, 195121 (2006).
- G. Orso, arXiv:cond-mat/0610437; H. Hu, X.-J. Liu and P. Drummond, arXiv:cond-mat/0610448.
- M.T. Batchelor, Physics Today **60**, 36 (2007).
- X.-W. Guan, M. T. Batchelor, C. Lee and M. Bortz, arXiv:cond-mat/0702191.